www.lajss.org
Latin American Journal of Solids and Structures 1 (2004)297–318

Identification of external loads in mechanical systems through heuristic-based optimization methods and dynamic responses

J.E. Rojas, F.A.C. Viana, D.A. Rade and V. Steffen, Jr*

Federal University of Uberlândia, School of Mechanical Engineering
2160 João Naves de Ávila Av., Campus Santa Mônica, CEP 38400-902, P.O. Box 593,
Uberlândia, Minas Gerais, Brazil

Abstract

This paper presents an inverse procedure for the determination of external loads, given the dynamic responses of the loaded structure and its corresponding finite element model. The influence of the stress-stiffening effect on the dynamic characteristics of structural systems is used to establish a relation between the dynamic responses and the applied external loading. An optimization problem is formulated in which the objective function represents the difference between the measured modal characteristics of the loaded structure and their finite element counterparts. The loading parameters (magnitude, position and direction) assumed as being unknown, are considered as design variables. The identification procedure is illustrated by means of numerical simulations, in which the identification problem is solved by using heuristic techniques coupled with classical optimization methods. Two heuristic techniques are considered, namely the LifeCycle Model and Particle Swarm Optimization. The classical optimization strategy is the Lagrange-Newton SQP (Sequential Quadratic Programming) method.

Keywords: Inverse problems, identification, LifeCycle model, Particle Swarm Optimization

1 Introduction

In the realm of Structural Engineering, it is very important to determine the external loading under real service conditions, aiming at evaluating the level of security of the structure, to verify the design configurations that were adopted at the design stage, or for redesigning structural elements for new operating conditions. However, the determination of external loading is not simple from the experimental point of view because, in general, transducers cannot be easily introduced in the structure during its construction and/or assembling. Consequently, in most real-life structures, experimental determination of external loading is not feasible.

By taking into account the influence exerted by the external loading on the dynamical response of the system through the so-called stress-stiffening effect, it is possible to obtain

* Corresponding author E-mail: vsteffen@mecanica.ufu.br Received 17 June 2004; In revised form 28 June 2004

information about the loading distribution, given the dynamic responses, through an inverse problem approach. Depending on the size of the structure, such a procedure presents a number of practical advantages:

- requires simple measurement and processing of dynamical responses by using a limited amount of sensors and signal conditioners;
- possibility of performing the measurement in various points along the structure, since the dynamic responses represent the global characteristics of the structure;
- availability of experimental techniques for excitation and data acquisition, as currently used in classical experimental modal analysis.

On the other hand, some difficulties that are intrinsic to inverse problems may arise, such as:

- it is required an accurate mathematical model of the structure, since the results of the identification procedure rely upon the mathematical model used;
- in general, identification problems are ill conditioned from the mathematical point of view. This means that the procedure is sensitive to noise that can contaminate experimental data;
- the experimental data are incomplete either in the spatial sense (responses are available only in a limited number of positions along the structure), as in the spectral sense (responses are obtained in a given frequency band). Consequently, the uniqueness of the solution cannot be assured.

In structural systems for which operation, integrity and security rely on the dynamic characteristics, the effect of external loading on the dynamic behavior of the system is to be carefully analyzed. The study of the dynamic behavior of mechanical systems can be done through numerical modeling techniques or by means of experimental modal analysis. Each technique exhibits its own hypotheses, limitations, advantages and disadvantages as shown in [18]. In this sense, parameter identification by model updating involves various steps and the main objective is to improve the model, in such a way that numerical results mimic those obtained from experimental testing.

Many modeling techniques are available, however the Finite Element Method - FEM is recognized as being the most flexible tool for structural analysis and for that reason has become very popular in the engineering community, as described in [38]. It is worth mentioning that, in parallel with the development of the finite element method, modal analysis techniques have been improved significantly in the past twenty years and are considered as being fairly reliable in determining the dynamic characteristics of mechanical systems. Parameter identification

methods and model updating techniques result from the necessity of constructing more reliable mathematical models, considering that finite element models and experimental models are only approximations of real structure behavior, as illustrated in [7].

It is well known the fact that external loads can influence the static and dynamic behavior of structural systems, through the so-called stress-stiffening effect [9, 17].

Reference [22] was the first one to put in evidence the effect of axial loads on the natural frequencies of structural components. In [28] it was recognized a common theoretical foundation underlying free vibration and stability analyses. In [35] the authors investigated the dynamic behavior of a clamped plate subjected to uniform membrane tension. In [4] it was demonstrated the existence of a linear relation between the axial load and the natural frequencies corresponding to the lateral motion of a simply supported column.

The changing of natural frequencies as related to stability problems was also discussed in the works reported in [36] and [3]. More recently other authors investigated analytically and experimentally the influence of axial loads on the vibration of beams under various boundary condition configurations [8, 34].

In [1] the authors demonstrated the possibility of introducing residual stresses as a mean to improve the mechanical behavior of thin plates. Further, Reference [12] showed that such stresses can be generated by piezoelectric actuators bonded to the plates. In [6] it was investigated the efficiency of piezoelectric actuators in controlling the natural frequencies of laminate plates through the introduction of membrane stresses.

In the context of inverse problems, Reference [16] used modal parameters combined with Least Squares to estimate the axial loads of Euler-Bernoulli beams having elastic supports. In [10] it was studied the effect of the application of an axial load to one of the bars in a truss structure by using experimental dynamic responses in a model fitting approach, in which the axial loads were considered as parameters to be adjusted. The results were then compared to the static loads as calculated from experimental measurements by using strain gages. The sensitivity analysis of the parameters to be adjusted has also been carried out. Besides, through experimental tests in a similar structure, Reference [15] analyzed the effect of residual stresses due to the construction process on the modal characteristics of the structure.

It is also important to mention the contribution from the work done by [19] in which it was investigated the influence of non-uniform temperature distribution on buckling and dynamic behavior of thin plates by using Rayleigh-Ritz approach.

More recently, [32] and [33] proposed a methodology for the identification of membrane stresses in rectangular thin plates from the transverse vibration responses, validating the procedure by numerical simulations and experiments. A particular application in this case was the determination of welding induced residual stresses.

There exist various techniques to solve inverse problems by using optimization methods, involving either classical as well as heuristic approaches. Once the parameters are identified, the mathematical model becomes an effective tool to analyze and predict the dynamics of the structure under different operating conditions.

It is well known that the solution of inverse problems by using classical gradient-based optimization methods is a difficult task due to the existence of local minima in the design space. Moreover, such methods require an initial guess to the solution and it is not possible to assure global convergence. These aspects have motivated the authors of this paper to explore a hybrid approach for the determination of external loading in structures, based on two heuristic methods, namely the LifeCycle model and the Particle Swarm Optimization (PSO) that were introduced in References [14] and [13] respectively, coupled with a classical approach to refine the local search in the optimum neighborhood. The Lagrange-Newton sequential quadratic programming (SQP) technique is used [29].

In this paper the optimization procedure uses modal parameters obtained through numerical simulation as "experimental values" in the objective function. Since this methodology is devoted to further experimental developments, it is important to take into account errors that arise in experimental modal analysis. Consequently, modal data are corrupted by random perturbations and the results are compared to those obtained for the case without noise.

The present contribution results from two previous recent conference papers, each of which focusing on one of the above mentioned heuristics [25, 26].

2 Dynamic modeling of two dimensional structures including the stress-stiffening effect

In this section it is briefly reviewed the finite element modeling of two-dimensional beam-like structures, according to the theory of Euler-Bernoulli, including the effect of the axial load, as illustrated in Figure 1.

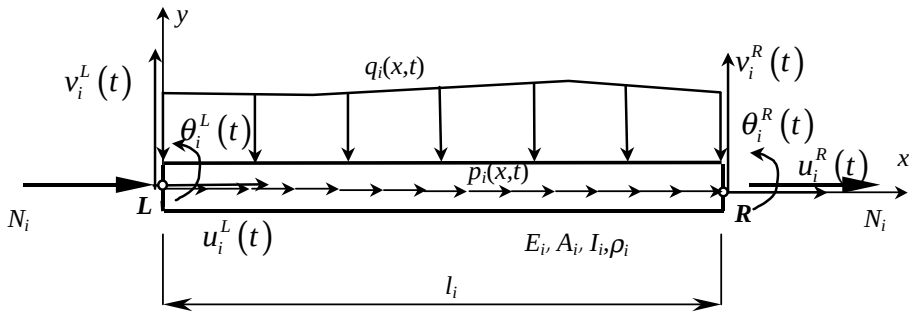

Figure 1: Two-dimensional beam element.

- u_i^Landu_i^R are the longitudinal nodal displacements,
- v_i^L andv_i^R are the transversal nodal displacements,
- $\theta_i^L$and θ_i^R are the nodal cross section rotations,

- l_i is the length of the element,
- E_i is the modulus of elasticity of the material,
- A_i is the area of the cross section,
- I_i is the area moment of inertia,
- p_i is the distributed longitudinal load,
- q_i is the distributed transversal load,
- N_i is the nodal load applied in the axial direction, equivalent (in the virtual work sense) to all the external loading.

The indexes L and R indicate, respectively, the displacements and rotations at the left hand and right hand nodes of the element.

Using a linear interpolation function to represent the longitudinal displacement and a cubical function for the transversal displacement, the following expressions for the element stiffness and mass matrices are obtained [5]:

$$K_i = \begin{bmatrix} \frac{E_iA_i}{l_i} & 0 & 0 & -\frac{E_iA_i}{l_i} & 0 & 0 \\ & \frac{12E_iI_i}{l_i^3} + \frac{6}{5}\frac{N_i}{l_i} & \frac{6E_iI_i}{l_i^2} + \frac{1}{10}N_i & 0 & -\frac{12E_iI_i}{l_i^3} - \frac{6}{5}\frac{N_i}{l_i} & \frac{6E_iI_i}{l_i^2} + \frac{1}{10}N_i \\ & & \frac{4E_iI_i}{l_i} + \frac{2}{15}N_il_i & 0 & -\frac{6E_iI_i}{l_i^2} - \frac{1}{10}N_i & \frac{2E_iI_i}{l_i} - \frac{1}{30}N_il_i \\ & & & \frac{E_iA_i}{l_i} & 0 & 0 \\ & & & & \frac{12E_iI_i}{l_i^3} + \frac{6}{5}\frac{N_i}{l_i} & -\frac{6E_iI_i}{l_i^2} - \frac{1}{10}N_i \\ sim & & & & & \frac{4E_iI_i}{l_i} + \frac{2}{15}N_il_i \end{bmatrix} \tag{1}$$

$$M_i = \frac{m_i}{420}\begin{bmatrix} 140 & 0 & 0 & 70 & 0 & 0 \\ & 156 & 22l_i & 0 & 54 & -13l_i \\ & & 4l_i^2 & 0 & 13l_i & -3l_i^2 \\ & & & 70 & 0 & 0 \\ & & & & 156 & -22l_i \\ sim & & & & & 4l_i^2 \end{bmatrix} \tag{2}$$

where $m_i = \rho_i A_i l_i$ and ρ_i represents the density of the material.

The effect of the axial load can be observed in the stiffness matrix at the elements corresponding to the bending stiffness, representing, therefore, the so-called stress-stiffening effect.

The global equations of motion are represented in the matrix form by (3):

$$\boldsymbol{M}\ddot{\boldsymbol{X}}(t) + \boldsymbol{K}(\boldsymbol{p})\boldsymbol{X}(t) = \boldsymbol{Q}(t) \tag{3}$$

where $\boldsymbol{p}$ is the vector of the axial loads applied to the beam elements that form the finite element model of the structure.

From the equations of motion, the following eigenvalue problem can be derived:

$$[\boldsymbol{K}(\boldsymbol{p}) - \lambda \boldsymbol{M}]\,\boldsymbol{X} = \boldsymbol{0} \tag{4}$$

where $\lambda = \omega^2$ is an eigenvalue (natural frequency) and $\boldsymbol{X}$ is an eigenvector (mode shape).

The matrix form of the frequency response functions (FRFs) is calculated as:

$$\boldsymbol{H}(\Omega) = \left[\boldsymbol{K}(\boldsymbol{p}) - \Omega^2 \boldsymbol{M}\right]^{-1} \tag{5}$$

where Ω is the excitation frequency.

The equations above show that the dynamic responses depend on the applied axial loads in the elements of the structure, which depend directly on the external load applied to the structure as a system. Before performing the dynamic analysis of the structure, a static analysis must be carried out to determine the axial loads for each element, as explained in [24].

3 Inverse problem formulation

The identification procedure to determine the external loads consists in solving a constrained optimization problem, in which the cost function represents the difference between the measured and model-predicted natural frequencies and/or the vibration mode shapes of the loaded structure. The magnitude, position and direction of the external loads (assumed as unknown) play the role of design variables.

In this way, one intends to obtain the loads to be applied in the model that optimally reproduces the experimental responses of the loaded structure.

For that purpose, the objective function used in this work is defined as:

$$J(\boldsymbol{p}) = \sum_{i=1}^{k} \left\{ W_\omega \frac{\left|\omega_i^{(m)}(\boldsymbol{p}) - \omega_i^{(e)}\right|}{\omega_i^{(e)}} + W_V \frac{\left\|\boldsymbol{V}_i^{(m)}(\boldsymbol{p}) - \boldsymbol{V}_i^{(e)}\right\|}{\left\|\boldsymbol{V}_i^{(e)}\right\|} + W_M \left\{1 - MAC\left[\boldsymbol{V}_i^{(m)}(\boldsymbol{p}), \boldsymbol{V}_i^{(e)}\right]\right\} \right\} \tag{6}$$

with the side constraints:

$$\boldsymbol{p}^L \leq \boldsymbol{p} \leq \boldsymbol{p}^U \tag{7}$$

where:

- $MAC\left[\boldsymbol{V}_i^{(m)}(\boldsymbol{p}), \boldsymbol{V}_i^{(e)}\right] = \left\{ \frac{\left[\boldsymbol{V}_i^{(m)}(\boldsymbol{p})\right]^T \boldsymbol{V}_i^{(e)}}{\left\|\boldsymbol{V}_i^{(m)}(\boldsymbol{p})\right\| \left\|\boldsymbol{V}_i^{(e)}\right\|} \right\}^2$ is the so-called Modal Assurance Criterion,
- m is the number of eigen-solutions used,

- $\boldsymbol{p}$ is the vector of external load parameters (to be identified),
- $\omega_i^{(m)}(\boldsymbol{p})$ and $\boldsymbol{V}_i^{(m)}(\boldsymbol{p})$ are natural frequencies and vibration mode shapes calculated from the finite element model, respectively,
- $\omega_i^{(e)}(\boldsymbol{p})$ and $\boldsymbol{V}_i^{(e)}(\boldsymbol{p})$ are experimental natural frequencies and vibration mode shapes of the loaded-structure, respectively,
- W_ω, W_V and W_M are weighting factors.

The side constraints are introduced to limit the values of the design variables within a feasible design space, avoiding the possibility of buckling or structural collapse due to extreme external load levels.

In the applications considered in this work, the cost function was constructed by using the first six modal parameters and limiting the value of the total load identified between zero and the first buckling load of the structure. Obviously, when the position and the directions of the load are to be identified, the design space becomes discrete and its dimension depends on the maximum number of nodes of the finite element model and the number of degrees of freedom for each node, respectively. The forth-coming applications illustrate different load configurations (magnitude, position and direction) that are characterized by increasing the number of load parameters to be identified, aiming at evaluating the influence of the number of unknown parameters in the performance of the identification procedure, as in [24]. Also, it is intended to present examples showing structures with different levels of complexity.

4 Particle Swarm Optimization

The social psychologist James Kennedy and the electrical engineer Russel Eberhart introduced the PSO in 1995 [13], as emerged from experiences with algorithms inspired in the social behavior of some bird species [21].

Consider the following situation: a swarm of birds is searching for food around a delimited area. Suppose there is just one place where food can be found and the birds do not know where it is. If a bird is well succeed in its search, it can attract other birds, and as a result of the social behavior, the others will find the food too. From the socio-cognitive viewpoint this means that mind and intelligence are social features, as demonstrated in [21]. Following this principle, each individual learns (and contributes) primarily to the success of his neighbors. This fact requires the balance between exploration (the capacity of individual search) and exploitation (the capacity of learning from the neighbors).

The essence is the learning from the experience of other individuals. From the optimization viewpoint, find the food is similar to reach the optimum. In this sense, the adjustment between exploration (the act of traveling around a place in order to learn about it) and exploitation (taking advantage of someone else's success) is required. If there is little exploration, the birds

will all converge on the first good place encountered. On the other hand, if there is little exploitation, the birds will never converge or they will try alone to find food. The individuals must be individualistic, as well as they have also to be able to learn from their neighbors in order to maximize their efforts in finding the best results [21].

4.1 A basic Particle Swarm Optimization algorithm

As shown in the previous section, the main idea of the PSO is to mimic the social behavior of birds, which are referred to as particles in the remainder. This is achieved by modeling the flight of each particle by using a velocity vector, which considers a contribution of the current velocity, as well other two parts accounting for the own knowledge of the particle and of the knowledge of the swarm about the search space. In this way, the velocity vector is used to update the position of each particle in the swarm [13, 21, 23, 30, 31, 37].

It can be seen in Figure 2 an outline of a basic PSO algorithm.

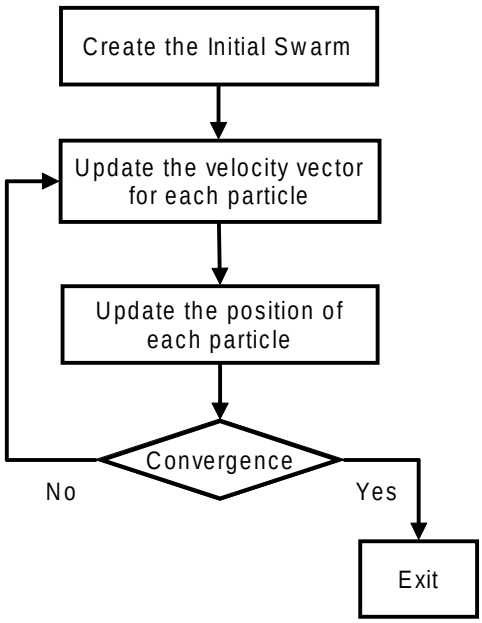

Figure 2: Basic PSO algorithm.

The position of each particle is updated according to the following equation:

$$x_{k+1}^{i} = x_{k}^{i} + v_{k+1}^{i}\Delta t \tag{8}$$

where, x_{k+1}^{i} is the position of the particle i in the iteration $k+1$, v_{k+1}^{i} is the corresponding velocity vector and Δt is the time step (it is assumed to be equal to one in this work).

The velocity vector is updated as follows:

$$v_{k+1}^i = wv_k^i + c_1 r_1 \frac{(p^i - x_k^i)}{\Delta t} + c_2 r_2 \frac{(p_k^s - x_k^i)}{\Delta t} \tag{9}$$

where r_1 and r_2 are random numbers between 0 and 1, p^i is the best position found by the particle i and p_k^s is the best position achieved by the remaining particles of the swarm in the iteration k.

There are three problem-dependent parameters, namely the inertia of the particle (w), and the two "trust" parameters c_1 and c_2. The inertia controls the exploration capacity of the algorithm: the larger the inertia value, the more global (as opposed to individualistic) will be the behavior [31]. The trust parameters indicate how a particle trusts on itself (c_1) and on the swarm (c_2). Figure3 shows the application of the equation above when two particles are flying in a bi-dimensional search space.

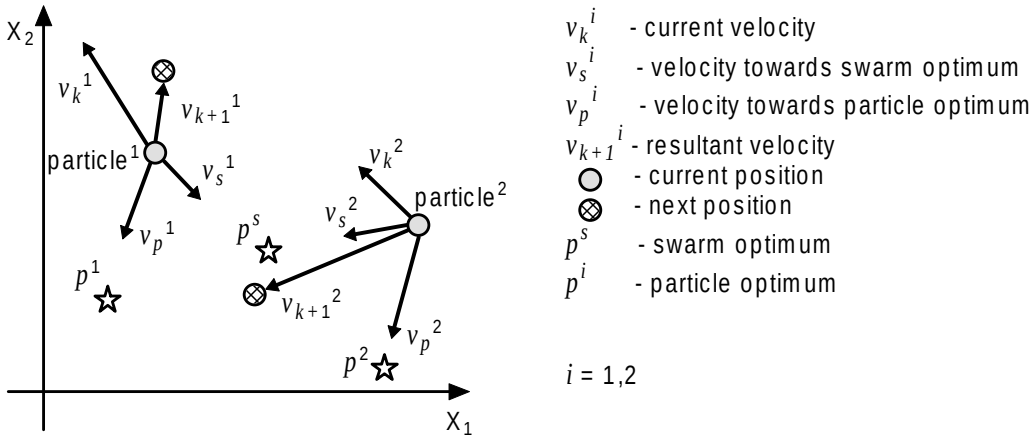

Figure 3: Velocity vector in action.

4.2 Initial swarm

The initial swarm is created by randomly distributing the particles throughout the search space. The initial position and the initial velocity vectors are given by the following equations:

$$x_0^i = x_{\min} + r_1(x_{\max} - x_{\min}) \tag{10}$$

$$v_0^i = \frac{x_{\min} + r_2(x_{\max} - x_{\min})}{\Delta t} \tag{11}$$

where r_1 and r_2 are random numbers between 0 and 1, $x_{\min}$is the lower bound vector and $x_{\max}$ is the upper bound vector for the variables.

4.3 Problem parameters

The formula used to update the velocity vector, Eq. (9), contains some parameters that are adjusted according to the problem, namely the trust parameters, c_1 and c_2, and the inertia weight, w. The trust parameters must be set to balance the influence of the knowledge that was acquired by an individual particle and the knowledge acquired by the swarm. The inertia weight is set to give the portion of the current velocity that will remain in the next iteration. The literature proposes using $c_1 = c_2 = 2$ and $0.8 \leq w \leq 1.4$ [13, 21, 23, 30, 31, 37]. In addition, the trust parameters can be set with different values, generally satisfying $c_1 + c_2 = 4$. In this work the values are $c_1 = 1.5$ and $c_2 = 2.5$. As for the inertia weight, a scheme of reduction is available, the so-called mass extinction [30, 31, 37]. The idea is to start with a large value for w, which provides a more global search, and then reduces continually the value during the optimization, providing a more local search behavior. This approach results in a faster algorithm convergence and makes the problem independent from the value assigned to w. The following equation gives the updating of w:

$$w_{new} = f_w w_{old} \tag{12}$$

where w_{new} is the updated value; w_{old} is the previous value and f_w is a constant between 0 and 1. $f_w = 0.975$ is used throughout this paper.

The w value is not updated each iteration. A coefficient of variation (CV) for a subset of the best particles is monitored. If CV falls below a pre-defined threshold value, it is understood that the algorithm is converging towards an optimum [31], then Eq. (12) is applied. The CV is given by the following equation:

$$CV = \frac{StdDev}{Mean} \tag{13}$$

where $StdDev$ is the standard deviation and $Mean$ is the mean of the objective function for the considered set of particles. In this work, a subset of the best 20% of particles from the swarm is monitored.

4.4 Dealing with Violated Constraints

When in an optimization problem the particles violate the constraints, they must be dealt with repairing such violation. As suggest by [31], the idea of feasible directions [29], is used to achieve this goal.

Consequently, the velocity vector is recomputed according to the equation:

$$v_{k+1}^i = c_1 r_1 \frac{(p^i - x_k^i)}{\Delta t} + c_2 r_2 \frac{(p_k^s - x_k^i)}{\Delta t} \tag{14}$$

After obtaining the new velocity vector, the position is recalculated by using Eq. (8). The difference between this formula and the initial one is that the current velocity is neglected. According to [30], in most cases this new velocity vector will bring the particle back to a feasible region of the search space.

4.5 Discrete/Integer Variables

The PSO algorithm and the Genetic Algorithm differ in this point, the first one was originally introduced to solve continuous problems and the second one was first introduced to solve discrete problems. However, an implementation of PSO algorithm to solve discrete problems is available. In this work, a simple modification is made by considering the position of each particle as an integer number. The approach is straightforward. The position of each particle is rounded to its closest integer value after applying Eq. (8) or Eq. (10). This method, although simple, was shown to be quite effective in the tested problems.

4.6 Craziness Operator

As the Genetic Algorithm has the mutation operator, the PSO algorithm has the craziness operator to avoid premature convergence. There are different ways to implement the craziness operator. In this work, the procedure suggested by [31] is adopted. The position is randomly changed while the velocity vector is recomputed following the equation:

$$v_{k+1}^{i} = c_1 r_1 \frac{(p^i - x_k^i)}{\Delta t} \tag{15}$$

This operator is applied to the particles that are identified by the previously defined coefficient of variation (CV), at the end of each iteration. If the CV falls below a pre-defined threshold value it is understood that the swarm is becoming too much uniform [31]. In this case, those particles located more than two standard deviations from the center of the swarm are subjected to the craziness operator. In this work a CV threshold of $thresh_{CV} = 1$ is used.

4.7 Stop criterion

The maximum number of iterations is defined previously and the algorithm runs until this number is reached. However, convergence criteria could be used, such as monitoring the maximum change in the objective function for consecutive iterations.

4.8 Simplifications and Enhancement to the Basic Algorithm

The goal of this work is to implement a basic algorithm that can be applied to solve constrained inverse problems. To achieve this goal, a simplification in consideration of the side constraints and a way to take into account the coefficient of variation (CV) that is adopted in the mass extinction and in the craziness operator, are introduced. When a particle violates a side constraint, its position is changed arbitrarily to a random value by applying Eq. (10). In [31] the procedure to compute CV includes the standard deviation ($StdDev$) and the mean value ($Mean$) of the objective function. Here, the position of each particle is monitored by the CV, instead. It is possible to exist particles that correspond nearly to the same value of the objective function but

occupy distant positions in the search space. In this way, the position of each particle is more significant than the value of its objective function.

In this work, the craziness operator was tested in the load identification problem. The results showed a worsening of the identification algorithm and because of that the PSO was implemented without the craziness operator.

5 The LifeCycle model

LifeCycle model is an optimization method based on artificial life (ALife) principles. The term Alife is used to describe the study of systems that have some essential features of life. ALife can be divided in two important topics:

- how computational techniques can help in biologic phenomenon studies.
- how biologic principles can help to solve computational problems.

In this context, the LifeCycle model is a computational tool inspired in the biologic concept of life cycle. From a biology viewpoint, the term is used here to define the passage through the phases during the life of an individual. Some phases, as sexual maturity, are one-time events, others, as the mating seasons, are re-occurring. Although it does not happen in every case, the transitions between life cycle phases are started by environmental factors or by the necessity to fit to a new condition [21]. The transition process promotes the maturity of an individual and contributes to the adaptation and evolution of its species.

From the optimization viewpoint, the capability of changing to a different stage by searching a way to improve the own fitness to the environment can be used to inspire a new optimization method. In this sense, the fitness provides a criterion used by each individual to shift its life stage. Different from what happens in genetic algorithms, where the natural evolution inspires the optimization method as a whole, in the LifeCycle model the transitions between the stages inspire just a part of the method. The transitions are used to deal with the mechanism of self-adaptation to the optimization problem. To close the definition, the LifeCycle stages must be defined. In the present work, two heuristics are used as stages, namely the GA and the PSO. Others versions of the LifeCycle model can be proposed by considering other heuristics and a mix of them as shown in [21]. This means that the optimization approach does not follow a rigid scheme as proposed in [2], in which various techniques are used sequentially in a cascade-type of structure.

5.1 Basic LifeCycle model algorithm

The outline of a basic LifeCycle algorithm is as follows:

1. Initialize the algorithm parameters for the PSO and GA.

2. Evaluate the fitness for all particles (PSO) and individuals (GA).
   If there is no recent improvement, switch the LifeCycle stage (change from GA to PSO or vice-versa).

3. For all PSO particles, run the PSO algorithm.

4. For all GA individuals, run the GA algorithm.

5. Go to step 2 and iterate until a stop criterion is achieved.

In the above LifeCycle model the algorithm is initialized with a set of particles of a PSO swarm, which can turn into GA individuals, and then, according to their performance, back to particles again and so on. A LifeCycle individual switches its stage when there is no fitness improvement for more than a previously defined number of iterations. In this work, this will be a parameter that can be adjusted according to the problem.

5.2 Parameters of LifeCycle model

Since the algorithm is composed by various heuristics, it is necessary to set the parameters of every heuristic used in the LifeCycle model. Nevertheless, there is a parameter inherent to the LifeCycle model, namely the number of iterations that represents a stage of the LifeCycle. The authors, to improve the algorithm performance, have introduced this parameter differently from what is usually done by simply fixing this number, as in [21]. We call this number as stage interval. At the end of each stage interval, the less well-succeeded individuals must change their stage in order to improve their fitness.

5.3 Stop criterion

In this work no convergence criterion is used. Simply, the number of iterations was defined previously and the algorithm iterates until this number is achieved. However, relative errors calculated for successive iterations can be used to stop the algorithm.

6 Genetic Algorithm

GA is an optimization algorithm based on Darwin's theory of survival and evolution of species, as explained in [11] and [20]. The algorithm starts from a population of random individuals, viewed as candidate solutions to the problem. During the evolutionary process, each individual of the population is evaluated, reflecting its adaptation capability to the environment. Some of the individuals of the population are preserved while others are discarded; this process mimics the natural selection in the Darwinism. The remained group of individuals is paired in order to generate new individuals to replace the worst ones in the population, which are discarded in the selection process. Finally, some of them can be submitted to mutation, and as a consequence, the

chromosomes of these individuals are altered. The entire process is repeated until a satisfactory solution is found.

The outline of a basic GA is as follows:

1. Define the GA parameters (population size, selection method, crossover method, mutation rate, etc.).
2. Create an initial population, randomly distributed throughout the design space (other distributions can be performed).
3. Evaluate the objective function and take it as a fitness measure of each individual.
4. Select mates to the crossover; this mimics the natural selection.
5. Reproduce and replace the worst individuals in the population by the offspring.
6. Mutate, to avoid premature convergence (other parts of the design space are explored).
7. Go to step 3 and repeat until the stop criterion is achieved.

Although the initial proposed GA algorithm was dedicated to discrete variables, nowadays, improvements are available to deal with discrete and continuous variables, see [11] and [20] for more details.

7 Sequential quadratic programming (SQP)

The linear search algorithm used in this paper is based on the Lagrange-Newton Sequential Quadratic Method (SQP) and is devoted to the minimization of a function of several variables $f(x)$,subjected to linear/non-linear equality and inequality constraints ($Ax \leq B$, $A_{eq}x = B_{eq}$, $Cx \leq 0$, $C_{eq}x = 0$) and side constraints ($l_b \leq x \leq l_u$). To obtain the optimal solution it is required an initial estimation of the optimization parameters [29]. Obviously, in the case of the present contribution, the results obtained from SQP depend on the initial estimation of the external forces and the number of variables to be identified.

8 Numerical Applications

8.1 Two-dimensional portal frame

Figure 4 shows a finite element model of a simple frame structure used in the identification process, which is submitted to four different load configurations. The identification problem consists in determining the loading parameters, namely the magnitude, position and direction.

The following scenarios are studied: 1- identification of the magnitude of $\boldsymbol{F}_1$; 2 - identification of the magnitude and position of $\boldsymbol{F}_1$; 3 - identification of the magnitude, position and direction of $\boldsymbol{F}_1$; 4 - identification of the magnitude and position of forces $\boldsymbol{F}_2$ and $\boldsymbol{F}_3$. Table 1 presents the natural frequencies with and without the external load for all studied scenarios.

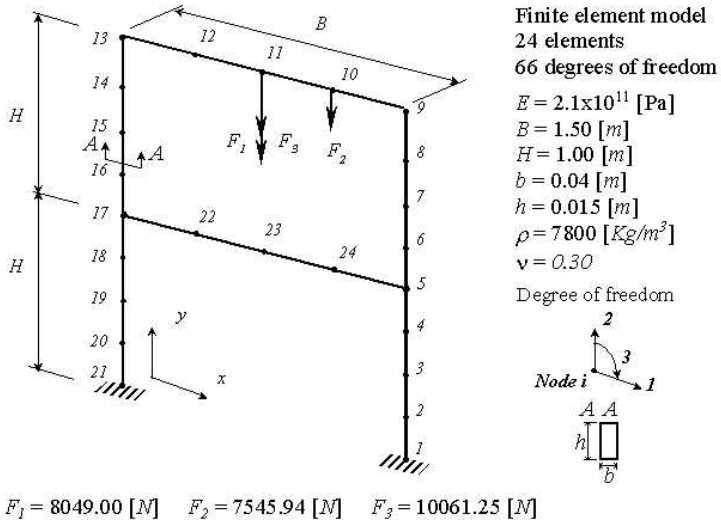

Figure 4: Portal frame structure FEM model (F_1 and F_3 are applied at the same position).

Table 1: Natural frequencies of the portal frame structure.

Scenario		Natural Frequencies [Hz]					
		1	2	3	4	5	6
Without load		4.42	15.07	22.74	28.30	51.85	59.64
1, 2, 3	$\boldsymbol{F}_1$ (N)	3.49	13.20	21.69	28.56	49.89	58.05
4	$\boldsymbol{F}_2$ and $\boldsymbol{F}_3$ (N)	1.66	10.59	20.34	28.71	47.30	56.22

The results obtained by using PSO and LifeCycle were used as an initial configuration for a second optimization run. This way the SQP method was used in this final step, thus forming a hybrid optimization approach. The most significant results of this approach are that the continuous design variables (force magnitudes) could be improved with respect to the previous step as obtained at the end of the PSO and LifeCycle runs.

Table 2 and Table 3 present the identification results to various loading configurations (scenarios) for the portal frame structure, as obtained by using PSO and LifeCycle model, respectively. As in real applications, identification methods have to be robust enough to deal with experimental errors, it is also considered a situation in which "experimental" data are corrupted with 10% of random error, as presented in Table 2 and Table 3. In the following tables $\boldsymbol{F}_i$ refers to the magnitude of the external loading and $\boldsymbol{P}_i$, $\boldsymbol{D}_i$ denote the position and direction of $\boldsymbol{F}_i$,

respectively.

Table 2: Identification results for the portal frame structure using PSO and PSO+SQP.

			Without corrupted data			With corrupted data			
			PSO	Hybrid		PSO		Hybrid	
Scenarios		Exact	Identified	Identified	Error [%]	Identified	Error [%]	Identified	Error [%]
1	$\boldsymbol{F}_1$ [N]	8049.00	8039.6098	8049.0043	$3.73\text{x}10^{-6}$	8826.3381	9.6575	8881.6772	10.345
2	$\boldsymbol{F}_1$[N]	8049.00	7742.55	8049.0034	$7.45\text{x}10^{-6}$	7552.7869	6.165	7552.7869	12.3875
	$\boldsymbol{P}_1$	11	11	-	0	11	0	-	0
3	$\boldsymbol{F}_1$[N]	8049.00	8465.32	8049.0043	$3.73\text{x}10^{-6}$	7822.2389	2.8173	7802.5716	3.0617
	$\boldsymbol{P}_1$	11	11	-	0	11	0	-	0
	$\boldsymbol{D}_1$	2	2	-	0	2	0	-	0
4	$\boldsymbol{F}_2$[N]	7545.94	7117.46	7545.95	$1.33\text{x}10^{-4}$	8014.89	6.21	7372.31	2.30
	$\boldsymbol{P}_2$	10	10	-	0	10	0	-	0
	$\boldsymbol{F}_3$[N]	10061.26	11387.70	10061.249	$1.09\text{x}10^{-4}$	10174.94	1.13	10423.92	3.60
	$\boldsymbol{P}_3$	11	11	-	0	11	0	-	0

Table 3: Identification results for the portal frame structure using LifeCycle and LifeCycle+SQP.

			Without corrupted data			With corrupted data			
			LifeCycle	Hybrid		LifeCycle		Hybrid	
Scenarios		Exact	Identified	Identified	Error [%]	Identified	Error [%]	Identified	Error [%]
1	$\boldsymbol{F}_1$[N]	8049.00	8053.03	8049.00	$2.76\text{x}10^{-5}$	8653.93	7.5156	8881.66	10.3448
2	$\boldsymbol{F}_1$[N]	8049.00	8278.40	8049.00	$4.73\text{x}10^{-5}$	8584.71	6.6556	9046.13	12.3882
	$\boldsymbol{P}_1$	11	11	-	0	11	0	-	0
3	$\boldsymbol{F}_1$[N]	8049.00	8044.98	8049.00	$5.05\text{x}10^{-5}$	8219.06	2.1127	7802.57	3.0616
	$\boldsymbol{P}_1$	11	11	-	0	11	0	-	0
	$\boldsymbol{D}_1$	2	2	-	0	2	0	-	0
4	$\boldsymbol{F}_2$[N]	7545.94	6547.86	7545.94	$5.12\text{x}10^{-5}$	8315.7	10.20	10345.60	6.8945
	$\boldsymbol{P}_2$	10	10	-	0	10	0	-	-
	$\boldsymbol{F}_3$[N]	10061.26	11023.11	10061.25	$6.73\text{x}10^{-5}$	9018.95	10.36	7025.69	2.8262
	$\boldsymbol{P}_3$	11	11	-	0	11	0	-	0

The behavior of the LifeCycle model along the iterations can be observed in Figure 5 for scenario 4, with noise. Figure 5-a shows the transitions due to its self-adaptation skills and Figure 5-b shows which heuristics is conducting the optimization process at a given iteration.

In the case illustrated in Figure 5, the stage interval is equal to 5 iterations; this means that transitions between PSO and GA happen at each group of 5 iterations. Since LifeCycle starts with PSO particles (in this case), in the first 5 iterations there are no GA individuals in the population. During the optimization process it can be observed that the LifeCycle individuals switch their stage (transition) to improve the value of the objective function.

The results show that both optimization approaches used in the force identification procedure were efficient for all scenarios analyzed. It is worth mentioning that both identification strategies lead to essentially the same results. As expected the identification errors are larger when corrupted data are considered. However, it can be seen that the methods are robust enough to provide meaningful results even in the presence of noise.

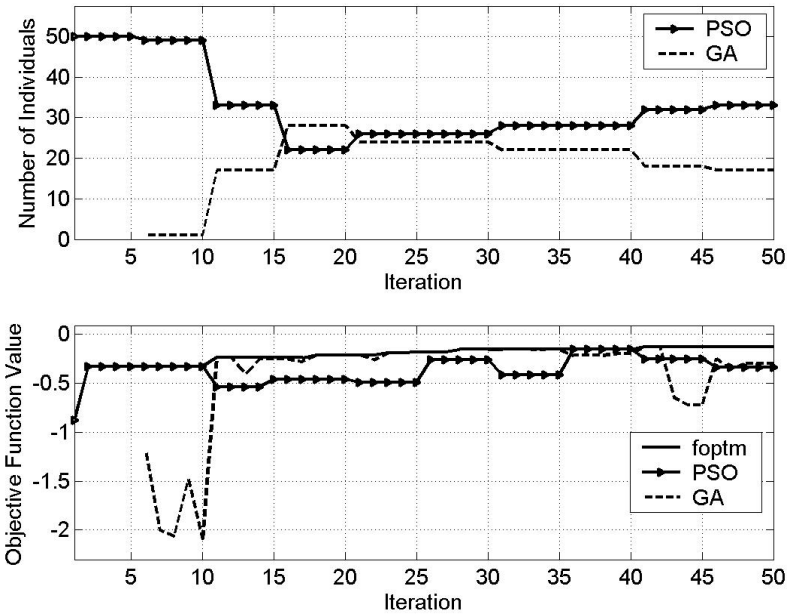

Figure 5: Evolution and performance of LifeCycle — portal frame structure.

8.2 Two-dimensional tower-like structure

Also, the authors intended to evaluate the efficiency of the identification algorithm when applied to a more complex finite element model. For this aim, a mechanical structure for which the first buckling load is 4669060 [N] is presented in Figure 6. In this case, the magnitude of a single force was determined (its position and direction were known a priori).

Table 4 presents the natural frequencies with and without the external load for the complex structure.

Table 4: Natural frequencies of the two-dimensional tower-like structure.

Scenario		Natural Frequencies [Hz]					
		1	2	3	4	5	6
Without load		29.51	82.12	145.49	161.58	217.74	333.44
1	$\boldsymbol{F}_1$[N]	23.50	62.48	111.83	161.39	175.81	315.47

Table 5 and Table 6 present the identification results for the complex structure for the two identification approaches studied in the present contribution, respectively. As in the previous case, "experimental" data were corrupted with 10% of random error for comparison purposes. Again, the results demonstrate the efficiency of the identification procedures.

As it was illustrated for the simpler structure (Figure 5), Figure 7 shows how the self-adaptation has performed in the complex structure case, when the LifeCycle approach was

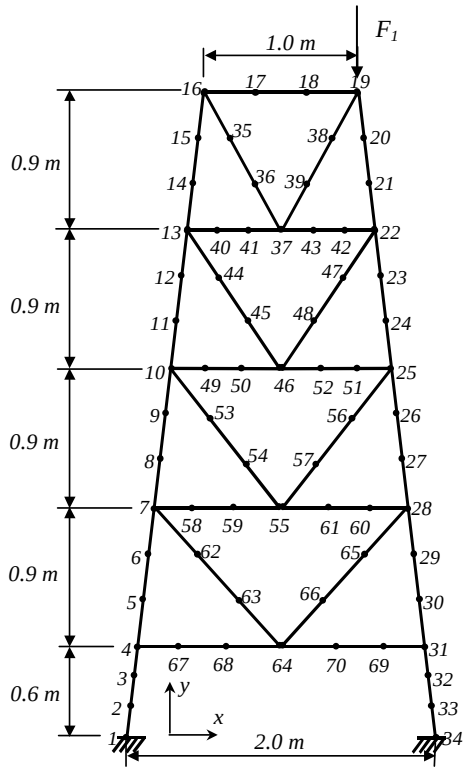

Figure 6: FEM of the two-dimensional tower-like structure.

Table 5: Identification results for the tower-like structure using PSO and PSO+SQP.

			Without corrupted data			With corrupted data			
			PSO	Hybrid		PSO		Hybrid	
Scenario		Exact	Optimum	Optimum	Error [%]	Optimum	Error [%]	Optimum	Error [%]
1	$\boldsymbol{F}_1$[N]	2334530.00	2352868.19	2364767.89	1.2952	2279644.7	2.351	2280107.1	2.3312

Table 6: Identification results for the tower-lie structure using LifeCycle+SQP.

			Without corrupted data			With corrupted data			
			LifeCycle	Hybrid		LifeCycle		Hybrid	
Scenario		Exact	Optimum	Optimum	Error [%]	Optimum	Error [%]	Optimum	Error [%]
1	$\boldsymbol{F}_1$[N]	2334530.00	2275699.84	2334529.84	$6.91\text{x}10^{-6}$	2276273.11	2.50	2364767.91	1.2952

used. The transitions between PSO and GA (Fig. 7-a) and the objective function value through the iterations (Fig. 7-b) can be seen.

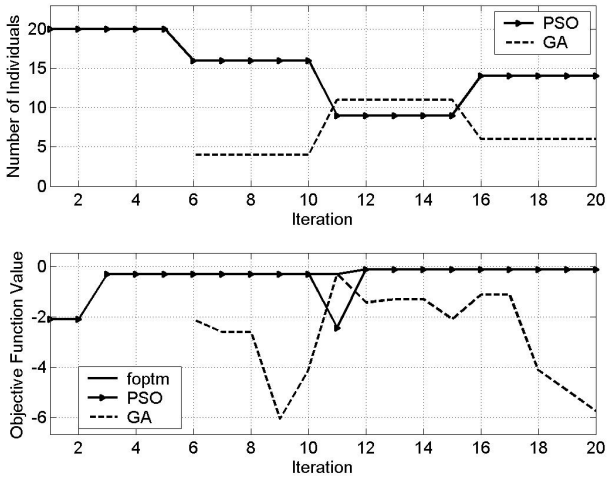

Figure 7: Evolution and performance of LifeCycle for the tower-like structure.

9 Conclusions

This paper presented an identification procedure to determine external forces applied to mechanical structures. Two identification strategies have been tested based on hybrid optimization methods as performed by PSO and LifeCycle model together with SPQ techniques. The influence of experimental errors was taken into account to test the robustness of the procedure. Various identification scenarios were investigated, in such a way that the efficiency of the identification procedure was checked in tests exhibiting increasing difficulty, ranging from a simple case in which a single force magnitude was determined to a configuration in which two force magnitudes and positions were obtained. In the cases for which the force positions were to be determined, the optimizer was able to deal with discrete design variables together with continuous ones. In most cases, the second optimization run using SPQ was very important to improve the results obtained, since heuristic techniques alone could not able to reach the global optimum. However, when corrupted data are used, SQP was no able to improve the results obtained from PSO and LifeCycle for all cases studied. This can be explained by the fact that SQP requires the computation of gradients of the cost function (partial derivatives). The corrupted data may locally increase the noise effect in calculating such derivatives, thus compromising the resulting optimal value obtained, as demonstrated in [27]. Random data errors smaller than 3influence the identification procedure. The results obtained are encouraging in the sense that real experimental data can be used in the near future to test the methodology developed under real-world

conditions.

Acknowledgments: Mr Rojas and Mr Viana are thankful to the Brazilian Research Agencies CAPES and CNPq, respectively for their graduate student scholarship. Dr Rade and Dr Steffen are grateful to CNPq to their research scholarships.

References

[1] S. F. M. Almeida and J. S. Hansen. Enhanced elastic buckling loads of composite plates with tailored thermal residual stresses. Journal of Applied Mechanics, 64(4):772–780, 1997.

[2] E.G. Assis and V. Steffen Jr. Inverse problem techniques for the identification of rotor-bearing systems. Inverse Problems in Engineering, 11(1):39–53, Taylor & Francis (2003).

[3] M. Baruch. Integral equations for nondestructive determination of buckling loads fos elastic plate and bars. Israel Journal of Technology, 11:1–8, 1973.

[4] T. H. Chu. Determination of buckling loads by frequency measurements. Master's thesis, Thesis at California Institute of Technology, 1949.

[5] R. R. Craig Jr. Structural dynamics: An introduction to computer methods. Wiley-Interscience, New York, page 544, 1981.

[6] S. F. M. Donadon, M. V. Almeida and A. R. Faria. Stiffening effects on the natural frequencies of laminated plates with piezoelectric actuators. Composites Part B-Engineering, USA, 33(5):335–342, 2002.

[7] M. I. Friswell and J. E. Mottershead. Finite Element Model Updating in Structural Dynamics. Kluwer Academic Publishers, Dordrecht, p.286, 1995.

[8] C. G. Go and C. D. Liou. Load-response determination for imperfect column using vibratory data. Journal of Sound and Vibration, 2002.

[9] P. D. Greening and N. A. J. Lieven. Modeling dynamic response of stressed structures. In Proceedings of the 17 th International Modal Analysis Conference, pages 103–108, Florida, 1999.

[10] P. D. Greening and N. A. J. Lieven. Identification and updating of loading in frameworks using dynamic measurements. Journal of Sound and Vibration, 260(1):101–115, 2003.

[11] R. L. Haupt and S. E. Haupt. Practical Genetic Algorithm. Wiley-Interscience, New York, 1 edition, 1998.

[12] S. F. M. Hernandes, J. A. Almeida and A. Nabarrete. Stiffening effects on the free vibration behavior of composite plates with pzt actuators. Composite Structures, Inglaterra, 49(1):55–63, 2000.

[13] J. Kennedy and R. C. Eberhart. Particle swarm optimization. In Proceedings of the 1995 IEEE International Conference on Neural Networks, pages 1942–1948, Perth, Australia, 1995.

[14] T. Krink and M. Løvberg. The lifecycle model: Combining particle swarm optimisation, genetic algorithms and hillclimbers. In Proceedings of the 7th International Conference on Parallel Problem Solving from Nature, pages 621–630, Granada, Spain, September 7-11 2002.

[15] N. A. J. Lieven and P. D. Greening. Effect of experimental pre-stress and residual stress on modal behavior. Philosophical Transactions of Royal Society London A 359, pages 97–11, 2000.

[16] J. G. Livingston, T. Béliveau and D. R. Huston. Estimation of axial load in prismatic members using flexural vibrations. submitted Journal of Sound and Vibration, 33(5):335–342, 1993.

[17] H. Lurie. Lateral vibrations as related to structural stability. Journal of Applied Mechanics, 19:195–204, 1952.

[18] N. M. M. Maia and J. M. Montalvão Silva. Theoretical and Experimental Modal Analysis. Research Studies Press LTD., England, p.468, 1997.

[19] D. J. Mead. Vibration and buckling of flat free–free plates under non-uniform in-plane thermal stresses. Journal of Sound and Vibration, 260:141–165, 2003.

[20] Z. Michalewicz. Genetic Algorithms + Data Structures = Evolution Programs. Springer-Verlag, New York, 2 edition, 1994.

[21] P. Pomeroy. An introduction to particle swarm optimization. http://www.adaptiveview.com, cited 15 September 2003.

[22] Lord Rayleigh. Theory of Sound, volume 2. Dover, New York, 2nd edition, 1989.

[23] S. Robinson, J. Sinton and Y. Rahmat-Samii. Particle swarm, genetic algorithm, and their hybrids: Optimization of a profiled corrugated horn antenna. In 2002 IEEE Antennas and Propagation Society International Symposium and URSI National Radio Science Meeting, San Antonio, Texas, June 2002.

[24] J. E. Rojas. Characterization of stress-stiffening effect and identification of loads in structures from dynamic responses. (in portuguese), M. Sc. Dissertation, Federal University of Uberlândia, Uberlândia-MG, Brazil, 2004.

[25] J. E. Rojas, F. A. C. Viana, D. A. Rade, and V. Steffen Jr. Force identification of mechanical systems by using particle swarm optimization (to be published). In Proceedings of the 10th AIAA/ISSMO Multidisciplinary Analysis and Optimization Conference, Albany, New York, Aug 30 – 01 Sept 2004.

[26] J. E. Rojas, F. A. C. Viana, D. A. Rade, and V. Steffen Jr. Force identification of mechanical systems through lifecycle model (to be published). In Proceedings of the ISMA2004 International Conference on Noise and Vibration Engineering, Leuven, Belgium, September 20-22 2004.

[27] D. A. Silva, L. A. Rade and J. Cunha. An assessment of genetic algorithms as applied to some inverse problems in elastodynamics. In Proc. of the 15^{th} Brazilian Congress of Mechanical Engineering - COBEM99, Águas de Lindóia, Brazil, November 21-26 1999.

[28] B. C. Stephens. Natural vibration frequencies of structural members as an indication of end fixity and magnitude of stress. Journal of the Aeronautical Sciences, 4:54–56, 1936.

[29] G. N. Vanderplaats. Numerical Optimization Techniques for Engineering Design. Vanderplaats Research and Development, Inc., 1999.

[30] G. Venter and J. Sobieszczanski-Sobieski. Multidisciplinary optimization of a transport aircraft wing using particle swarm optimization. In Proceedings of the 9th AIAA/ISSMO Symposium on Multidisciplinary Analysis and Optimization, volume AIAA 2002-5644, Atlanta, GA, September 4-6 2002.

[31] G. Venter and J. Sobieszczanski-Sobieski. Particle swarm optimization. In Proceedings of the 43rd AIAA/ASME/ASCE/AHS/ASC Structures, Structural Dynamics, and Materials Conference, volume AIAA-2002-1235, Denver, CO—USA, April 22-25 2002.

[32] A. B. Vieira Jr. Identification of Stresses in Rectangular Plates from the Vibration Responses with application to Welding Residual Stresses. Doctorate thesis (in portuguese), Federal University of Uberlândia, Uberlândia, MG, Brazil, 2003.

[33] A. B. Vieira Jr. and D. A. Rade. Identification of stresses in plates from dynamic responses. In Proceedings of IMACXXI - Conference and Exposition on Structural Dynamics, CD-ROM, 2003.

[34] L. N. Virgin and R. H. Plaut. Effect of axial load on forced vibrations of beams. Journal of Sound and Vibration, 168(3):395–405, 1993.

[35] A. Weinstein and W. Z. Chien. On the vibrations of a clamped plate under tension. Quaterly of Applied Mathematics, 1:61–68, 1943.

[36] W. H. Wittrick. Rates of changes of eigenvalues, with reference to buckling and vibrations problems. Journal of the Royal Aeronautical Society, 66:590–591, 1962.

[37] W. Xie, X.F. Zhang and Z. Yang. Hybird particle swarm optimizer with mass extinction. In Proceedings in the International Conference on Communication, Circuits and Systems (ICCCAS02), volume AIAA-2002-1235, pages 1170–1173, Chengdu, China, June 26-28 2002.

[38] O. C. Zienkiewicz and R. L. Taylor. The Finite Element Method, volume 1 and 2. McGraw-Hill, New York, 4th. edition, 1989.